I&EC research
Industrial & Engineering Chemistry Research

Article

pubs.acs.org/IECR

Structure and Strength of Flocs of Precipitated Calcium Carbonate Induced by Various Polymers Used in Papermaking

Roger Gaudreault,*[,†,‡,§] Nicolas Di Cesare,[†] Theo G. M. van de Ven,[‡] and David A. Weitz[§]

[†]Cascades Inc., Recherche et Développement, 471 Marie-Victorin, Kingsey Falls, Quebec Canada, J0A 1B0

[‡]Pulp & Paper Research Centre, McGill University, 3420 University Street, Montreal, Quebec Canada, H3A 2A7

[§]Harvard University, Pierce Hall 231, 29 Oxford Street, Cambridge, Massachusetts 20138, United States

ABSTRACT: Because of persistent economic pressure on cost reduction, inorganic fillers such as precipitated calcium carbonate (PCC) have become increasingly economically attractive in the papermaking process. The increase of filler level in paper can be achieved by adding it to pulp prior to the headbox, either as individual filler particles or as preaggregates, while maintaining paper strength and minimizing their negative impact. Consequently, the floc structure and strength of PCC aggregates was studied using flocculants and dry strength agents, using static light scattering/diffraction (SLS), real time fluorescent video imaging (RTFVI), image analysis, photometric dispersion analysis (PDA), and scanning electron microscopy (SEM). It was found that PEO/cofactor induced PCC aggregates were weaker at high shear and far more irreversible than those induced by the partially hydrolyzed polyvinyl formamide copolymerized with acrylic acid (PVFA/NaAA) or cationic starch. Flocs produced at low polymer dosages were smaller and weaker than those produced at higher dosages. The number of discrete PCC particles in aggregates was measured using real time fluorescent video imaging combined with image analysis. Finally, we speculate that when two scalenohedral crystal type PCC particles aggregate, there is a small effective surface area to bind them, mainly through classical bridging or charge neutralization flocculation. Moreover, additional polymer adsorption results in higher coverage of the external and internal surfaces and prevents further aggregation due to electrosteric repulsion.

INTRODUCTION

Because of persistent economic pressure on cost reduction, additives other than cellulose fibers, such as inorganic fillers, have become increasingly attractive components in the papermaking process. Typical filler addition levels range from 3% to 30%.[1] While most fillers are naturally occurring minerals, others are manufactured or engineered using chemical processes. The most common inorganic fillers are[1] kaolin clay, calcium carbonate, titanium dioxide, talc, silica, and silicate. These fillers are generally divided into two categories: (1) mineral fillers that are cheaper than fiber (regular and delaminated clays, ground calcium carbonates (GCC), precipitated calcium carbonates (PCC) and talc) and (2) specialty fillers that are more expensive than fiber and are used for more specific purposes (titanium dioxide, precipitated silica, silicates, as well as structured clays).[1] PCC is produced in scalenohedral, rhombohedral, and needle shaped or aragonite structures, with scalenohedral PCC being the most widely used in the wet end of papermaking. Aragonite can be produced in different ways and interestingly by changing the sequence of addition in the Kraft causticizing process.[2] Pouget et al.[3] showed that the initial stages of template-controlled $CaCO_3$ formation start with prenucleation clusters with dimensions of 0.6 to 1.1 nm (step 0). Aggregation of theses clusters in solution leads to the nucleation of amorphous calcium carbonate (ACC) nanoparticles with a size distribution centered around 30 nm (step 1). Association of these particles with the template surface initiates the growth of ACC (step 2), using the nanoparticles in their neighborhood as feedstock. Next crystallization starts, resulting in the formation of poorly crystalline particles (step 3). Randomly oriented nanocrystalline domains are formed inside the otherwise amorphous particles (step 4). In the last steps, the orientation that is stabilized through the interaction with the monolayer becomes dominant (step 5) and develops into a single crystal (step 6). This single crystal probably grows by the further addition and incorporation of ions and clusters from solution. Gebauer et al.[4] speculate that the release of water molecules from the hydration shell of ions provides a substantial entropy gain favoring prenucleation cluster formation. Piana et al.[5] used metadynamics to explore the free energy surface for ion diffusion across the $CaCO_3$ surface. Obviously, our work occurs at a much larger scale and is described later in this manuscript.

Fillers are generally added to pulp prior to the headbox, or as a coating applied to the surface of sheet once it is already formed. Although each type of filler has specific characteristics and fulfills particular functions, their role in the pulp and paper industry can be summarized as follows: (1) to reduce production cost (fiber substitution); (2) improve optical properties (opacity, brightness); (3) improve printability (ink holdout, greater levels of gloss, and better image quality); (4) improve sheet uniformity; (5) improve surface smoothness; and (6) improve dimensional stability.[1] However, fillers may have negative effects: (1) reduce mechanical strength (interference with interfiber bonding); (2) abrasion (on wires, blades and printing plates); (3) impair retention (increase of retention aid dosage); (4) increase two-sidedness; (5) reduce stiffness; (6) increase dusting tendency; (7) increase the quantity of deposits in the paper machine

Received: March 2, 2015
Revised: May 15, 2015
Accepted: May 29, 2015

DOI: 10.1021/acs.iecr.5b00818
Ind. Eng. Chem. Res. XXXX, XXX, XXX−XXX

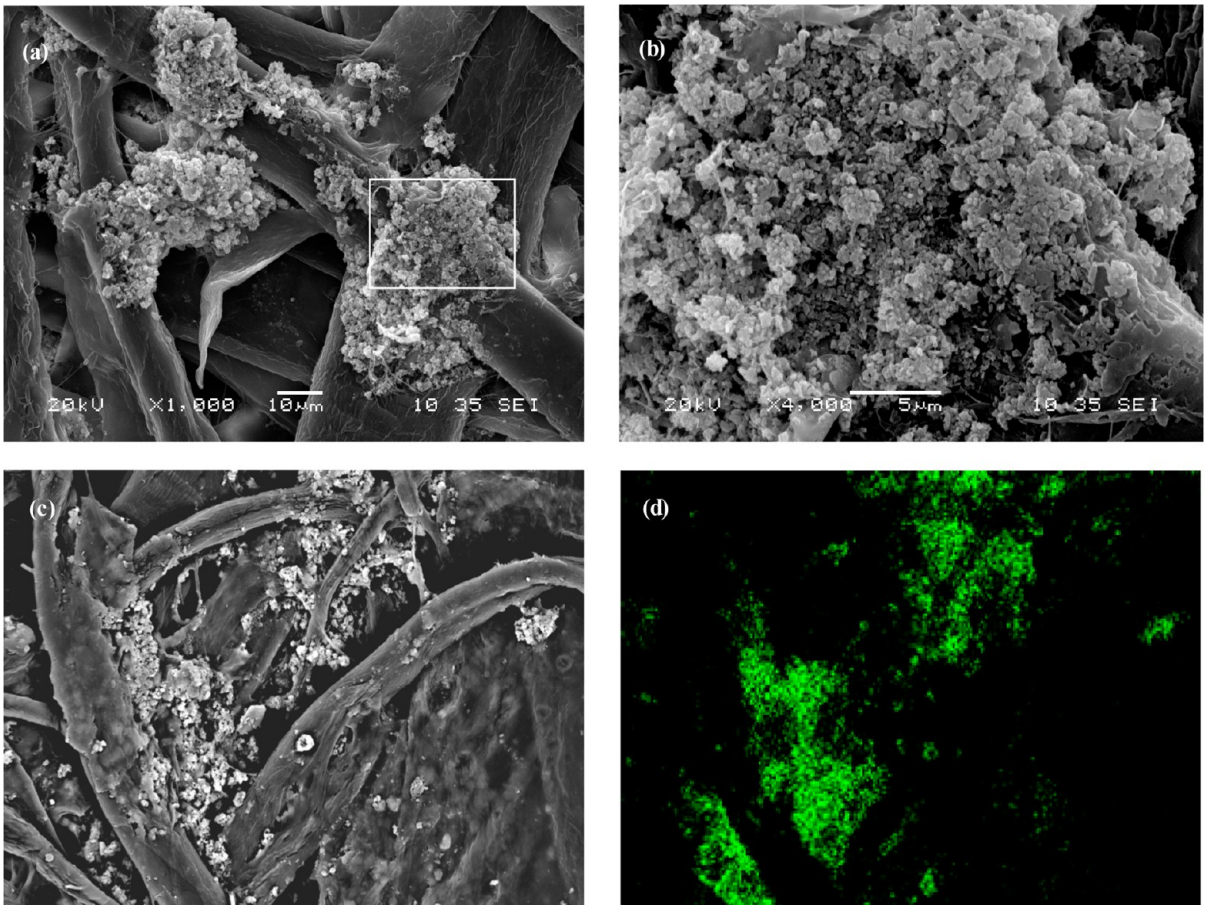

Figure 1. (a) SEM pictures showing filler aggregates in fine paper grade made from recycled fibers. (b) The picture on the right is an enlargement of a floc seen on the left. (c) SEM and (d) SEM/X-ray mapping of calcium in the filler aggregates.

system; and (8) require a more complex white water recirculation loop. Some fillers are more detrimental to paper strength than others. When compared at constant total area of filler per mass of paper, the burst strength follows the trend; clay > talc > GCC.[6,7] Similar strength effects were shown for GCC and PCC[8] whereas, at a subtler level, it seems that prismatic PCC is less detrimental to strength than scalenohedral PCC.[9,10]

Filler shape, aspect ratio, average particle size, size distribution, aggregate size, density, and specific surface area are critical parameters that determine paper properties. The smallest fillers have the most detrimental effect on paper strength, for a given filler type and a given dosage.[11,12] Bown[13] studied sheet properties with 20% filler content using chalk and kaolin having particle sizes of 1 to 12 μm. He showed the effect of aggregating kaolin to produce either a rigid, open structure (calcined kaolin) or a flexible, compressible structure (strongly flocculated kaolin).[13] Different methods showed that the filler distribution in paper sheets is irregular in the z (thickness) direction.[14−16] This reflects the complex influences of paper machine design, operational conditions, drainage, wet end chemistry, etc. Beazley and Petereit[6] published the most widely quoted model for filler strength effects which employs the specific surface area as the only filler property. However, Li et al. reported that their conclusion was valid only within a narrow range of filler types.[11]

Fillers weaken paper by lowering the fiber−fiber bonded area.[11,17] One possibility is that filler particles act as flaws, causing local areas of stress concentration, which initiate sheet failure.[18] Tanaka et al.[17] showed that the addition of potato starch improves the strength properties of nonfilled sheets made solely from Kraft pulp, without changing the structure, whereas beating or addition of filler changes their structure. Many authors have studied possible methods to introduce calcium carbonate fillers, and/or calcium carbonate composites, in pulp or paper and their effects on the optical and physical properties.[19−30] Several patents have been issued regarding the increase of calcium carbonate filler level in paper.[31−37]

Fillers often form aggregates well before sheet consolidation, especially in the short circulation loop of the paper machine.[38] Laboratory studies showed that (i) potato and tapioca starches were able to aggregate PCC, using deionized and process water at 50 °C, (ii) tapioca starch gave the highest rate of PCC aggregation and aggregate size compared to potato starches,[39] and (iii) the increase of collision efficiency at higher tapioca starch dosage was probably due to a more significant increase in the effective diameter of PCC particles.[40]

The proportion of the filler that will persist in real papermaking conditions as aggregates is still an open question. However, Figure 1 clearly shows that filler aggregates are present in fine paper. Figure 2 shows an undesirable situation where the filler particles, in a white top liner, are not uniformly distributed, which could negatively alter the optical properties of paper. However, this could strengthen the paper properties at identical filler concentration. Numerous SEM pictures were taken from different locations of a linerboard process (white top liner) and filler aggregates were observed all across the papermaking process, i.e., from the pulper to the end product (paper).

DOI: 10.1021/acs.iecr.5b00818
Ind. Eng. Chem. Res. XXXX, XXX, XXX−XXX

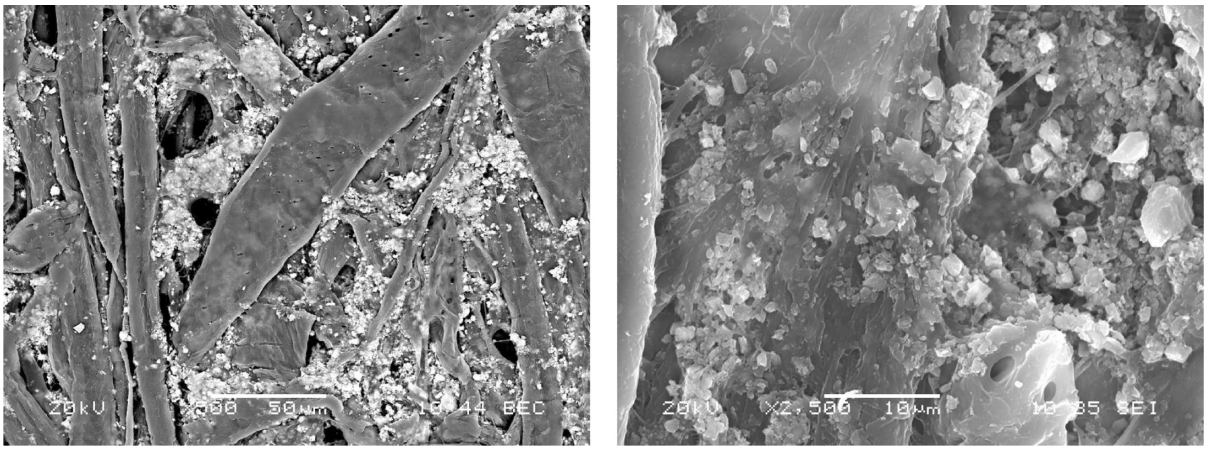

Figure 2. SEM pictures showing filler aggregates in white top linerboard.

Interestingly, the size of the aggregates was increasing as the pulp samples were taken closer to the headbox of the paper machine. This can probably be explained by the flocculating agents added prior to the headbox and by the flocculation of the originally nonretained fillers, which can then be incorporated as aggregates in the sheet, that occurs in the short circulation loop.[38,41] The challenge is to find the best compromise between the optical and strength properties of paper.

Macromolecules adsorbed onto the colloidal particle surface may either stabilize or destabilize the dispersions. The behavior will depend on the degree of surface coverage, molecular weight, charge density, type of polymer, and degree of dissolution. For partially covered surfaces, the already adsorbed polymer on a given particle may attach to the bare surface on another one, forming a particle−particle bridge (bridging flocculation).[42−46] The bridging flocculation mechanisms have been extensively studied.[42−51]

An important question is how can aggregation be induced to give a specific type of aggregate? The kinetics of interactions probably plays a critical role in the type of aggregates that can be created. Polymer type, concentration and experimental conditions can be adjusted to create open or dense aggregates. Two distinct limiting regimes of irreversible colloid aggregation (without shear) have been identified: "Diffusion-Limited Colloid Aggregation" (DLCA) giving open aggregates and "Reaction-Limited Colloids Aggregation" (RLCA), giving dense aggregates.[52−60] Each one has its own characteristic dynamics and produces aggregates with different fractal dimensions (d_f) where the mass of aggregate scales as a^{d_f} ($M \approx a^{d_f}$). DCLA implies an aggregation efficiency (α) of one, and RCLA to $0 < \alpha < 1$. Both can occur in papermaking.[38] Lin et al.[56−60] showed the universality of DLCA and RLCA. DLCA was studied by increasing the ionic strength of the system to ensure that the system is only limited by diffusion and not by electrostatic repulsion. RLCA is the opposite, in the sense that the colloids are aggregating at a slow rate due to the presence of electrostatic charges, or other interactions, thus giving dense aggregates. Lin et al.[56] used gold (a = 7.5 nm), silica (a = 3.5 nm), and polystyrene (a = 19 nm) to demonstrate the universality in colloid aggregation. They showed a striking similarity in the structure of the clusters of the different colloids in each regime: RCLA, resulting from slow coagulation, gave d_f = 2.1; DCLA, which covers rapid coagulation, gave d_f = 1.75.[56] Fast aggregation occurs between particles with the same sign at high salt concentration, or for oppositely charged particles. Weitz et al.[57] set the limits for the fractal dimension for irreversible kinetics aggregation of gold colloids, as $1.75 \leq d_f \geq 2.05$ (± 0.05). In terms of flocculation efficiency (α, $W = 1/\alpha$) one would expect that low flocculation efficiency would result in denser aggregates and higher fractal dimension, whereas high flocculation efficiencies would give open aggregates, i.e., lower fractal dimension. The above two phenomena are different from the aggregation of large PCC particles, which is shear induced.[61] Nevertheless, they parallel each other in the sense that it might be possible to control the experimental conditions to obtain open or dense aggregates. In papermaking, both perikinetic (diffusion controlled) and orthokinetic (shear induced) interactions are present, although most PCC aggregation will be shear induced.

Yilmaz and Alemdar developed a technique, based on steady state fluorescence measurements, to study cluster−cluster aggregation and sedimentation kinetics of organoclay.[62] They reported that pyranine was used as a fluoro-surfactant (bridging effect) and argued that the fluorescence intensity during the sedimentation process can be used to measure the fractal dimension of the aggregates as a function of organoclay concentration.[62]

However, none of the above publications report measurements of floc strength directly. Strength was inferred from the relationship between mixing intensity and retention.

The pioneering work using direct micromechanical measurements of floc strength showed that (i) there was no correlation between floc size (6 to 40 μm) and floc tensile strength (20 to 200 nN); (ii) two breakup mechanisms, depending upon floc structure: (a) surface erosion or (b) cohesive failure/large scale fragmentation; and (iii) very low strength when fractured flocs were put back together.[63,64]

The direct micromechanical measurements of floc strength (including PCC/cofactor) showed that) (i) PEO molecular weight (2 to 8 million Dalton) has an enormous effect on floc strength (10 to 130 nN), (ii) there is a large range in elasticity (fracture toughness) depending upon cofactor types (sulfonate containing phenolic resin and a linear copolymer of vinylphenol and sodium acrylate), and (iii) polymers that give the highest retention also make the strongest flocs.[65,66]

In our previous work, the kinetics of PCC aggregation was studied and compared with theoretical models.[61] It was found that the flocculation efficiency depends on the PCC surface area that can participate in bridging (bridging surface area), i.e., the surface area associated with the most protruding surface asperities. This surface area is much smaller than the total

DOI: 10.1021/acs.iecr.5b00818
Ind. Eng. Chem. Res. XXXX, XXX, XXX−XXX

surface area available for polymer adsorption. We proposed that the effective bridging surface area, which can form bonds between PCC particles or aggregates, should be used to study the kinetics of PCC aggregation, and not the total or projected surface area.[61]

In this work, we studied the properties of the final PCC flocs (aggregates) and correlate them with the type of polymer and with the flocculation kinetics studied earlier.[61] PCC aggregation was studied using static light scattering/diffraction (SLS), real time fluorescent video imaging (RTFVI), photometric dispersion analysis (PDA), image analysis, scanning electron microscopy (SEM), and light microscopy. Moreover, the reversibility and the strength of the aggregates, as well as the type of aggregates, were investigated.

Part of this work appears in the proceedings of the 14th FRC Symposium, Advances in Pulp & Paper Research, Oxford, U.K. (2009).[67]

MATERIALS AND METHODS

Chemicals. *Precipitated Calcium Carbonate (PCC).* Precipitated calcium carbonate (Albacar-HO from Mineral Technology Inc.) was used. The weak negative charge density of −1.3 mequiv/kg (ionic charge of the slurry: −272 μequiv/L) was measured for a 20.9% suspension of PCC sampled from the satellite production plant, without dilution. The pH of the PCC

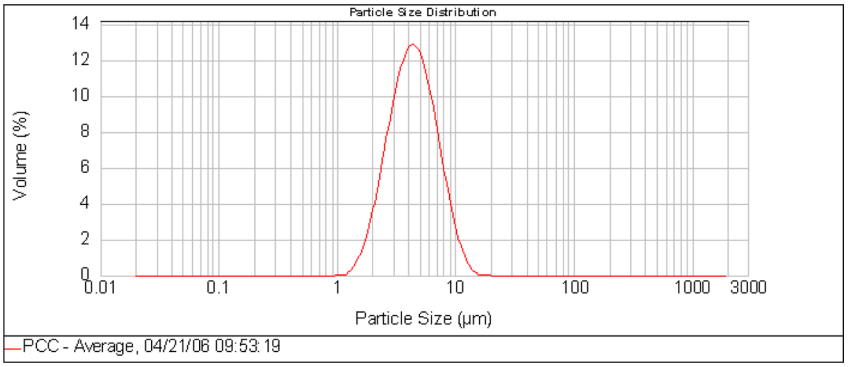

Figure 3. Particle size distribution of scalenohedral PCC measured by static light scattering/diffraction (SLS).

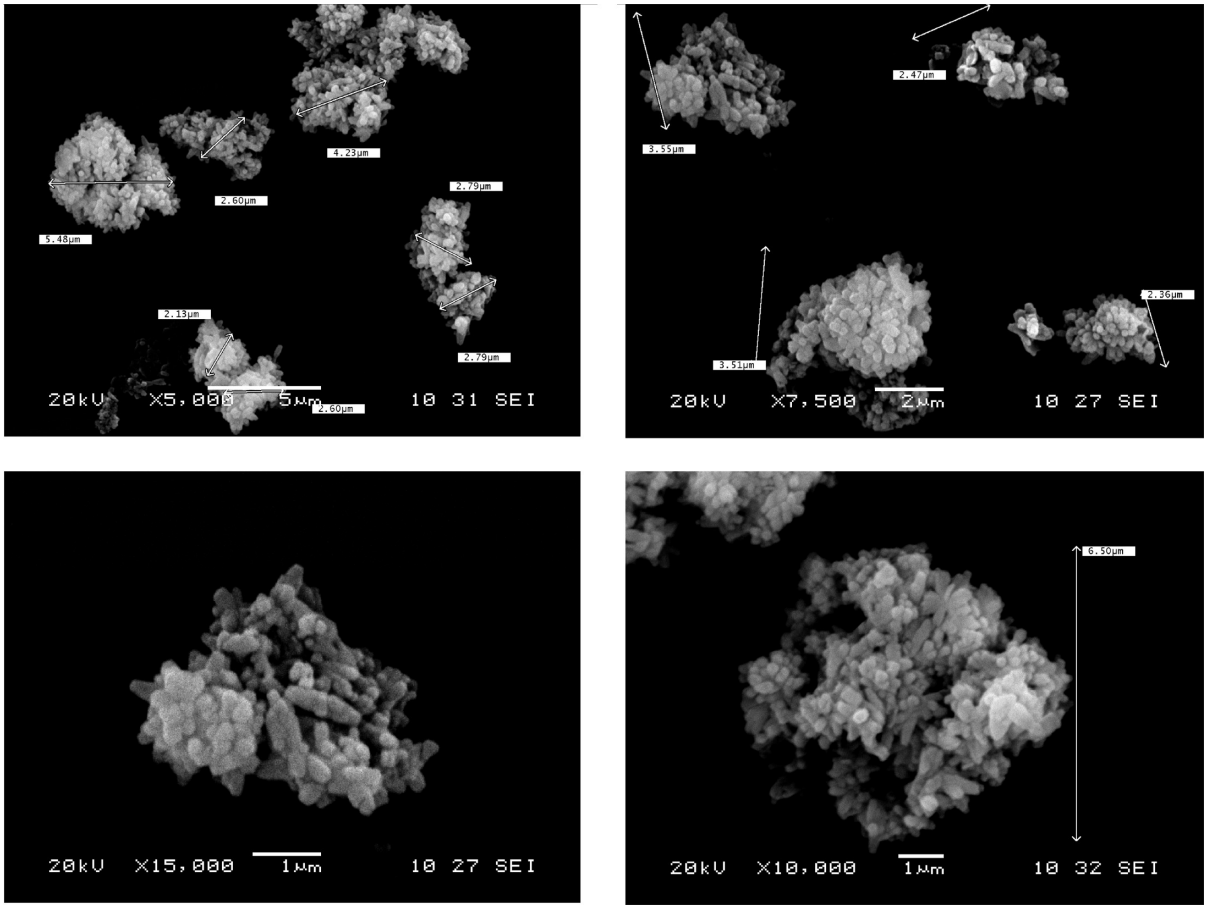

Figure 4. Typical SEM images of PCC particles in the original commercial 20.9% suspension.

DOI: 10.1021/acs.iecr.5b00818
Ind. Eng. Chem. Res. XXXX, XXX, XXX−XXX

Table 1. Characteristics of the Chemical Compounds

product	commercial name	charge density (equiv/kg dry)	description
cationic potato starch (C-starch)	EmCat C3 (AKP Canada Inc.)	+0.48	0.3% nitrogen
poly(ethylene oxide) (PEO)	Oxicol (Ciba Specialty Chemicals)	nonionic	$M_w \approx 6$ MDa
cofactor	Oxirez (Ciba Specialty Chemicals)	anionic	sulphone type resin
PVFA/NaAA	Catiofast PR 8236 (BASF)	amphoteric −1.2 (pH 9.0)	sodium salt of partially hydrolyzed polyvinyl formamide copolymerized with acrylic acid. $M_w \approx 0.6$ MDa
polyethylenimine (PEI)	Polysciences Inc.	+13.1 (pH 7.0) +5.5 (pH 9.0)	$M_w \approx 70$ KDa

suspension was 9.0. Pure PCC is positively charged,[68] as confirmed by molecular modeling calculations,[69] but turns negative upon dilution by adsorbing impurities, even in distilled water,[68] and it also turns negative in papermaking process water. The average particle size, measured by static light scattering/best fit diffraction pattern without constraint, is 4.4 μm (Figure 3). Measurements with and without ultrasound gave very similar PCC particle sizes.

Because these results were higher than those measured by sedimentation (1.43 μm), SEM was performed to validate them. The SEM pictures were obtained by taking one drop of stirred 20.9% PCC suspension and diluting it to 1/1000 to ensure discrete particles. Results showed the PCC particles to be irregular in shape, having lots of asperities, within the same size range as that measured by SLS/diffraction (Figures 3 and 4). The experimental specific surface area (SSA), measured by nitrogen adsorption, was reported to be 13.95 ± 0.70 m^2/g PCC by the supplier (2-year average).

Polymers. The polymers used to flocculate PCC are in Table 1, together with their charge density and some other properties. For all commercial dry polymers, including PEO, fresh solutions were prepared the day of experiment. Starch was cooked at 95 °C for 45 min at 2% (w/w) solids. After the cooking time, the starch was diluted with water and kept warm (40−45 °C) during the experimental work. All polymers were dissolved using deionized water.

Adsorption Isotherm. The adsorption isotherms were measured to determine the maximum amount of polymer adsorbed on the slightly negative PCC.[61] Two different chemistries were evaluated using (a) sodium salt of partially hydrolyzed PVFA/NaAA, an amphoteric polymer (Table 1, Figure 5) and (b) cationic potato starch, because it is commonly used in papermaking processes (Table 1).

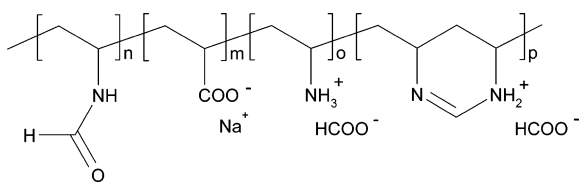

Figure 5. Molecular structure of the sodium salt form of partially hydrolyzed polyvinyl formamide copolymerised with acrylic acid (PVFA/NaAA).

Results showed that both chemistries yielded high affinity type adsorption isotherms, with a maximum amount of adsorbed polymer of: $\Gamma_{max} \approx 7$ mg/g PCC.[61] The Γ_{max} of PVFA/NaAA on PCC was validated and found to be identical to that of an external laboratory, using photometric titration (UV−vis spectrophotometer) methods (ref: BASF, Germany).

Even though the chemistry differs, polyethylenimine (PEI) has been shown to adsorb on GCC and PCC and adsorption isotherms after 1 h of equilibration gave Γ_{max} in the range of 4−10 mg PEI/g of PCC, depending on the particle size, surface area, and electrophoretic mobility.[70] Our results are within their range.

Particle Size Analyzer (Static Light Scattering/Diffraction). Particle size analyses were performed using a Malvern Mastersizer instrument equipped with a Hydro 2000S wet dispersion accessory (A). Static light scattering/diffraction (SLS) uses the full Mie theory to calculate the particle size. A refractive index of 1.607 was used for PCC. Results for PCC and PCC/polymer systems are an average of five measurements, with a stirring rate of 1925 rpm and no ultrasound.

Photometric Dispersion Analyzer (PDA). Aggregation. Changes in the state of PCC aggregation were monitored by a Photometric Dispersion Analyzer (PDA 2000 Rank Brothers, Cambridge, U.K.).[71,72] The PCC suspension was pumped from the outlet of a 1-L beaker through a transparent 3 mm diameter tubing into the photocell of the PDA, which monitors the fluctuations in intensity of transmitted light. The experimental apparatus and the mathematical background of this method for the measurements of the flocculation and breakup kinetics has

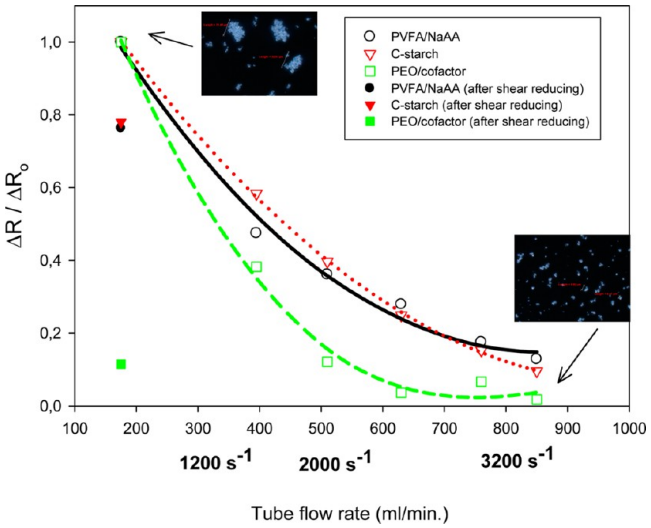

Figure 6. Normalized changes in apparent particle size ($\Delta R/\Delta R_0$) as a function of shear rate (s^{-1}) and as flow rate (mL/min) for different polymer treatments: 5 mg PVFA/NaAA/g of PCC; 2 mg C-starch/g of PCC; and 0.03125 mg PEO/0.143 mg cofactor/g of PCC; cofactor/PEO ratio of 4.5:1. The PCC concentration was 1g/L, temperature was room temperature, no salt was added, and the stirring rate was 300 rpm. Solid symbols show the apparent particle size after the shear was reversed from high to low level. Top left and bottom right pictures show the PEO/Cofactor/PCC aggregates under the lowest and highest shear rate, respectively.

DOI: 10.1021/acs.iecr.5b00818
Ind. Eng. Chem. Res. XXXX, XXX, XXX−XXX

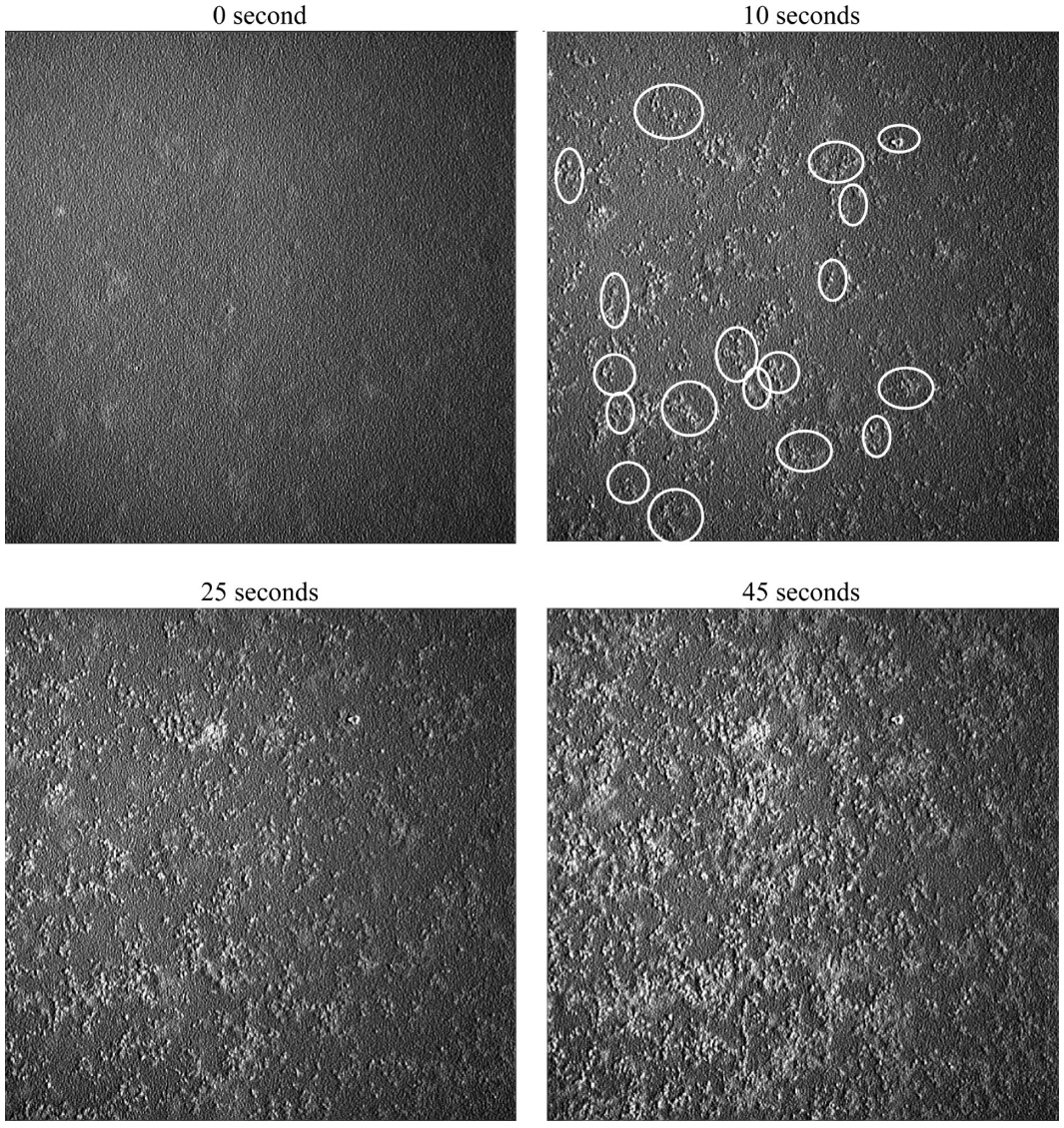

Figure 7. Accumulation of PCC aggregates on the bottom of the cuvette as a function of time. Experimental conditions: 1940 ppm PCC, 1 mg PVFA/NaAA/g PCC, 1 mM $CaCl_2$, and room temperature. Selected large aggregates are indicated by the circles. These images were enhanced to improve the contrasts.

been described in previous work.[61] Moreover, the changes in R (ΔR) correlate with changes in size (Δa) measured by static light scattering/diffraction.[61] This technique is ideal to measure the breakup of aggregates and hence their floc strength.

Microscopy and Real Time Fluorescent Video Imaging (RTFVI). Fluorescent images were acquired on a Leica DM-IRB inverted microscope equipped with a Hamamatsu intensified charge-coupled device (EB-CCD) camera C7190−21 (Hamamatsu City, Japan), and automated image acquisition software (Metamorph: Universal Imaging Corporation, Downington, PA). Polymer was tagged with an aldehyde reactive fluorescent probe, Alexa Fluor 488, to ensure proper visualization. Alexa Fluor 488 (Invitrogen Inc.) and PVFA/NaAA (0.05% w/w) were stirred together for 1 h in deionized water. The solution was then dialyzed for 12 h using a 3500 Mw cutoff membrane to remove any free probes. The fluorescent polymer is used to visualize PCC aggregation. Salt ($CaCl_2$) was added to the PCC suspension to simulate the papermaking process. Shear is only applied during a few seconds after the addition of salt and polymer to the PCC suspension. Salt ($CaCl_2$) and polymer were added simultaneously. Once the aggregation process has been initiated, about 1−1.2 mL of the suspension was poured into a small cuvette, without agitation. The estimated time between the injection of the chemicals (salt ($CaCl_2$) and polymer), and the imaging is about 10 s; results were corrected accordingly. This real time fluorescent video technique has the advantage of being able to visualize PCC aggregation. Two images were recorded every second, for at least 2 min or more, during an experiment. However, the experimental set up leads to the settling of the PCC aggregates, which makes interpretation of the particle size difficult. Various experimental conditions were attempted to overcome this, e.g., more aggregation leads to more and faster settling. Numerous PCC concentrations were explored: from 0.1 to 2500 ppm, and the optimum was found to be between 1580 and 1780 ppm. From this method, combined with image analysis, an attempt was made to measure the average number of discrete PCC particles in an aggregate, as a function of time, which is valuable information in the study of the kinetics of PCC aggregation. To get accurate information, the video images

DOI: 10.1021/acs.iecr.5b00818
Ind. Eng. Chem. Res. XXXX, XXX, XXX−XXX

were treated to improve the contrasts, using the sharpen mode of ImageJ software.

Image Analysis. For experiments (1 mg and 5 mg PVFA/NaAA/g of PCC), video images were taken from 0 to 45 s. These images were analyzed using image analyzer software (Clemex Vision PE version 3.5). A number of large aggregates were selected using the interactive mode of the image analyzer software. The area of particles was divided by the total area of the image, giving the fractional surface area covered by PCC particles or aggregates. Then, the fractional coverage area was plotted as a function of time.

RESULTS

Strength and Reversibility of PCC Aggregates. *Strength of PCC Aggregates (PDA Experiments).* PDA experiments were performed to show the relative intrinsic strength of PCC aggregates. On the basis of previous results,[61] the dosages of the chemicals (PVFA/NaAA, C-starch, and PEO/Cofactor) were selected to get a similar particle size at the lowest shear rate. Figure 6 shows the normalized apparent PCC aggregate size, expressed as $\Delta R/\Delta R_0$, under different shear rates, and where ΔR_0 is the PCC apparent particle size at the lowest shear rate. The mean shear rates (in reciprocal seconds) were calculated from the volumetric flow rate, Q, using the following:

$$G = \frac{8Q}{3\pi r^3} \tag{3}$$

where Q is the flow rate, and r is the radius of the inner diameter of the flexible tubing (3 mm).

Larger aggregates (higher ratio, ΔR) imply stronger aggregates and less breakup under the same shear rate. Figure 6 shows that, generally, the aggregate strength is similar when they are induced by PVFA/NaAA and starch, while the PEO/cofactor system gives somewhat weaker aggregates at high shear rates. It is worth mentioning that the current cofactor/PEO ratio is 4.5:1, while Goto and Pelton,[73] using a different cofactor, reported that the maximum scalenohedral PCC floc strength corresponded to a ratio of 2−3:1. They found that the flocs broke up when exerting an extensional force of about 100−140 nN. Results from Figure 6 show again that a dynamic equilibrium exists between the formation and breakup of aggregates at steady state. The reversibility of the aggregates was verified by measuring the ΔR after reversing the high shear rate back to the low shear rate. Figure 6 shows that PVFA/NaAA and starch-induced aggregation are partially reversible, while PEO/cofactor induced aggregation is not reversible.

Microscopy and Video Imaging. Numerous real time videos in fluorescent mode were performed to study the kinetics of PCC aggregation. Figure 7 shows typical images from 0 to 45 s, for the 1 mg PVFA/NaAA/g of PCC, 1 mM $CaCl_2$ system. Because of the way the experiments were performed, it was not obvious if the images in Figure 7 result from PCC aggregation and/or sedimentation at the bottom of the cuvette on the glass lamella. Consequently, the fractional surface area covered by the PCC was measured as a function of time (Figure 8). During sedimentation, the PCC flux toward the glass lamella surface is $j = nv$, n is the number of particles per unit volume, and v is the velocity. Hence, the fractional surface coverage, the surface occupied by the PCC out of the total surface, is $S = \pi a^2 jt$, t being the time. Substituting for v, the Stokes sedimentation velocity, and expressing n in terms of concentration, c, yields the following:

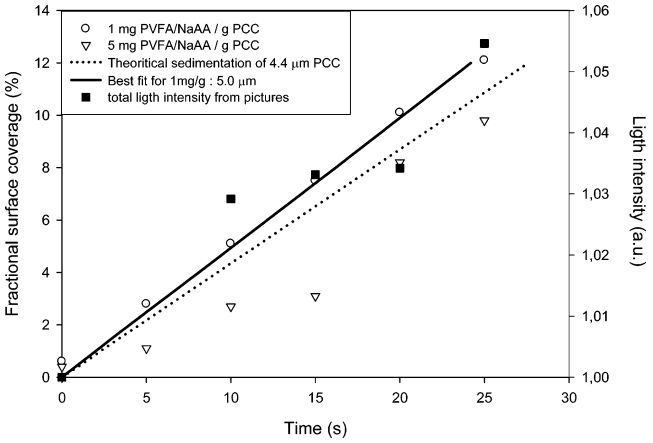

Figure 8. Fractional surface coverage and light intensity as a function of time. PCC was treated with 1 mg PVFA/NaAA/g of PCC (1940 ppm of PCC), and 5 mg PVFA/NaAA/g of PCC (1780 ppm of PCC). Both experiments were performed at 1 mM $CaCl_2$ and room temperature. Dashed line shows the theoretical sedimentation for nonflocculated PCC. The best fit (solid line) corresponds to a PCC of 5.0 μm.

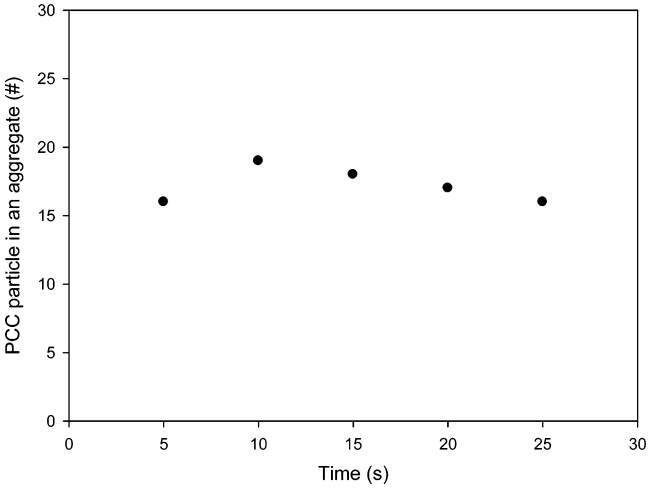

Figure 9. Experimental average number of discrete PCC particles in selected large aggregates as a function of time. The data to build this graph are not statistical average. Experimental conditions: 1780 ppm PCC, 5 mg PVFA/NaAA/g PCC, 1 mM $CaCl_2$, and room temperature.

$$S = \frac{gac\Delta\rho t}{6\eta\rho_{PCC}} \tag{4}$$

where g is the gravitational acceleration, a the PCC radius, c the PCC concentration, $\Delta\rho$ the density difference ($\rho_{PCC} - \rho_{H_2O}$), ρ_{PCC} the density of PCC, η the viscosity of water, and t the time. Equation 4 predicts that the fractional surface area should increase linearly with time. Indeed, Figure 8 shows that S is linearly related to time and supports that sedimentation is the main mechanism for the 1 mg PVFA/NaAA/g PCC system ($r^2 = 0.9999$ for 1 mg PVFA/NaAA/g PCC). Moreover, Figure 8 shows that the best fit for the radius of PCC is 5.0 μm, larger than the 4.4 μm of the nonaggregated PCC, implying that a small amount of aggregation has occurred. Because the estimated time between the injection of chemicals ($CaCl_2$ and PVFA/NaAA) and the imaging is about 10 s, this is about the amount of aggregation you can expect in such a short time. Stopping the shear is equivalent to quenching the aggregation.

DOI: 10.1021/acs.iecr.5b00818
Ind. Eng. Chem. Res. XXXX, XXX, XXX−XXX

Furthermore, the light intensity was measured to validate the above trend and to see if polymer adsorption can be measured with this technique. Even though the light intensity follows the same trend as the fractional surface area, very few data points are available, and a lot more experiments are needed to draw any conclusion.

This method, combined with image analysis may be used to estimate the number of discrete PCC particles in an aggregate. For example, the PVFA/NaAA system at a dosage of 5 mg/g of PCC and 1 mM $CaCl_2$ shows the average number of discrete PCC particles in selected large aggregates to be about 17−18 (Figure 9). Because this technique is exploratory and very time-consuming, large aggregates were selected to demonstrate its usefulness. Consequently, Figure 9 does not intend to give a statistical average. More work is needed to demonstrate the potential of this new method.

Type of Aggregates. Whether open or dense aggregates are suitable for papermaking is not clear yet, but we can speculate that the open aggregates would be better, at least for the optical properties of paper, because of the larger surface area to scatter more light.

The chemical additives were added into a 1 L dispersion of 1000 ppm of PCC. The suspension was stirred for 5 min at 300 rpm using a 3 cm propeller before an aliquot was taken for image

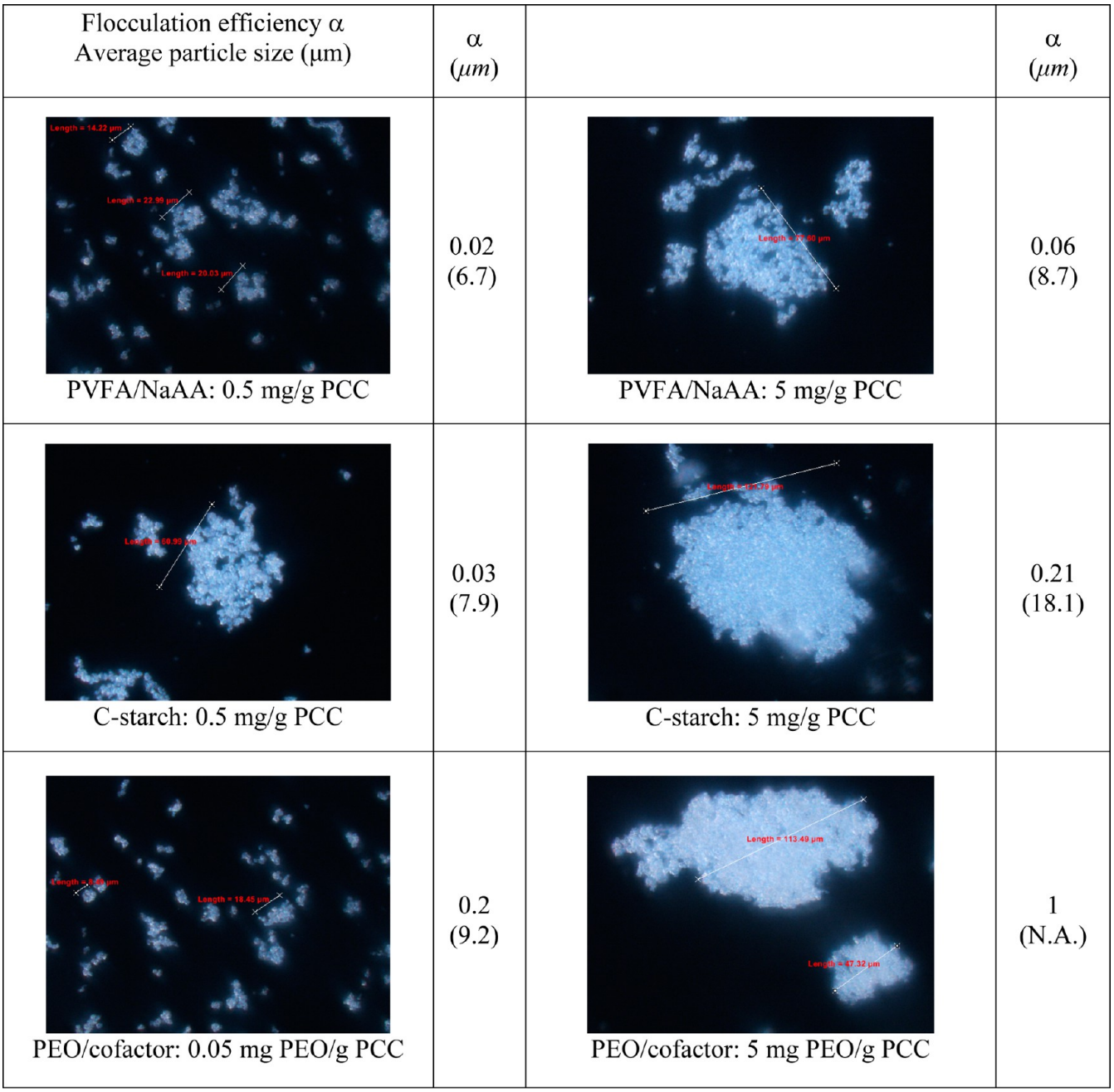

Figure 10. PCC floc sizes for low and high dosages of PVFA/NaAA (0.5 and 5 mg/g PCC), C-starch (0.5 and 5 mg/g PCC), and PEO/Cofactor (0.05 and 5 mg of PEO/g PCC). The cofactor/PEO ratio, 4.5:1, was constant for both PEO dosages. The flocculation efficiency (α, $W = 1/\alpha$) and the statistical average particle size were taken from Figures 11 and 12.[61] However, these parameters do not correlate with the above pictures because only one floc or a few flocs are shown. Reproduced with permission from FRC, copyright 2009, under the Berne Convention and the International Copyright Convention. Published by The Pulp and Paper Fundamental Research Society.

DOI: 10.1021/acs.iecr.5b00818
Ind. Eng. Chem. Res. XXXX, XXX, XXX−XXX

recording. Image recording was performed 1 to 4 h after flocs reaction. The dispersions were manually gently shaken, and 100 μL was placed on a microscope glass slide. A cover glass was carefully deposited on the drop, and the excess of water was removed with absorbent paper. Photos were taken using dark field illumination.

Figure 10 compares the PCC floc structures and sizes for low and high dosages of PVFA/NaAA (0.5 and 5 mg/g PCC), C-starch (0.5 and 5 mg/g PCC), and PEO/Cofactor (0.05 and 5 mg of PEO/g PCC). These three chemical systems were selected from previous work because they cover a wide range of aggregate sizes.[61] PEO/cofactor systems show fast aggregation, generating large aggregates of about 23 μm with 1 mg/g of PCC; C-starch shows intermediate aggregation rates and floc sizes; and PVFA/NaAA systems show a slower aggregation rate and aggregate sizes of 5−8 μm (Figure 11).

From Figures 11 and 12, it can be seen that low dosages lead to low flocculation efficiencies and smaller flocs, whereas high

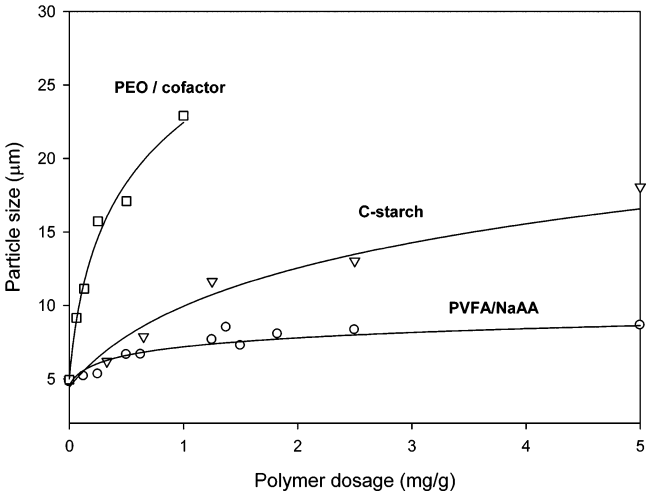

Figure 11. Particle size as a function of polymer dosage. All experiments were performed using 2000 ppm of PCC suspensions, room temperature, no added salt, and a mean shear rate of 10^3 s^{-1}. The cofactor/PEO ratio, 4.5:1, was constant for all PEO dosages. Reproduced with permission from FRC, copyright 2009, under the Berne Convention and the International Copyright Convention. Published by The Pulp and Paper Fundamental Research Society.

dosages lead to higher flocculation efficiencies and larger flocs, which is consistent with Sang and Englezos.[40] For low dosages, the size of the flocs is due to a dynamic equilibrium between floc formation and breakup, because there is sufficient room for further bridging and flocs should grow without limit if breakup was absent. For higher dosages, the floc size may be determined by a competition between polymer adsorption and particle aggregation. Flocs form before the filler surface is fully saturated by the polymer, and subsequent polymer adsorption prevents further floc growth because of electrosteric repulsion between the PCC particles.[68] This implies that the floc strength increases with polymer dosage. This explains the difference in floc size for the two dosages in Figure 10. However, from the floc images, it is hard to conclude whether flocs get denser or not when they get larger (Figures 10 and 13). Larger flocs contain more particles, many of which overlap in an image. Moreover, the density of flocs depends on the shear history of the flocculation process, and flocs often get denser at high shear.[74−78] This densification could be more pronounced for larger flocs because the hydrodynamic forces exerted on them are larger. This might be the reason why

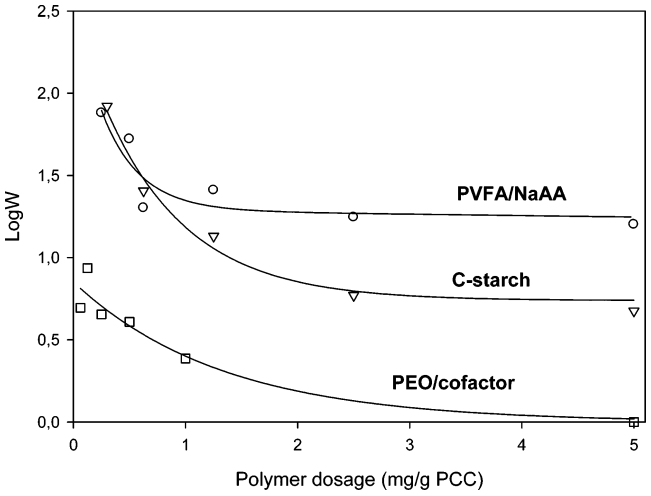

Figure 12. Stability ratio (Log W) as a function of polymer dosage. All experiments were performed using 2000 ppm of PCC suspensions, room temperature, no added salt, and a mean shear rate of 10^3 s^{-1}. The fastest aggregation rate (W = 1, Log W = 0), obtained from the 5 mg PEO/cofactor/g of PCC system, was used as the reference aggregation rate to compare the performance of the above chemicals on the same basis. Reproduced with permission from FRC, copyright 2009, under the Berne Convention and the International Copyright Convention. Published by The Pulp and Paper Fundamental Research Society.

there is no obvious correlation between the flocculation efficiencies and floc densities, as is the case for perikinetic coagulation (Figures 10−13). More recently, Rasteiro et al.[79] looked at PCC flocs resistance and reflocculation, while others investigated PCC flocculation using cationic polyelectrolytes having different charge densities or ionic strength.[80]

The log W values did not rise again when the dosage was increased beyond an optimum point, likely because of transient aggregation, which was irreversible under the experimental conditions (Figure 12). Similar transient aggregation of PCC with CPAM was observed by Vanerek et al.[68]

Representative examples of floc sizes induced by C-starch for low and high dosages are shown in Figure 13.

Proposed Mechanism. From the above results and previous work,[61] we speculate that when two scalenohedral crystal type PCC particles aggregate, there is a small effective area to bind them (Figure 14). This effective area is much smaller than the projected surface area. The implication of this observation is that the experimental SSA, e.g., obtained from BET, cannot be used for the kinetic calculations because a significant amount of polymers is buried inside the asperities (dark green areas in Figure 14).

From the above pictures, model polymers were added to partially cover these scalenohedral crystal type PCC particles, where the cationic polyelectrolyte binds with the slightly anionic PCC particle, mainly through electrostatic interactions (top of Figure 15). Then, the other part of the cationic polyelectrolyte (e.g., loop, tail) interacts with the binding sites of another PCC particle (top of the surface asperities, light green), showing classical bridging or charge neutralization flocculation. Then, additional polymer absorption results in higher coverage of the external and internal surfaces and prevents further aggregation due to electrosteric repulsion (bottom of Figure 15).

■ CONCLUSIONS

PCC aggregation was studied using static light scattering/diffraction (SLS), real time fluorescent video imaging (RTFVI),

DOI: 10.1021/acs.iecr.5b00818
Ind. Eng. Chem. Res. XXXX, XXX, XXX−XXX

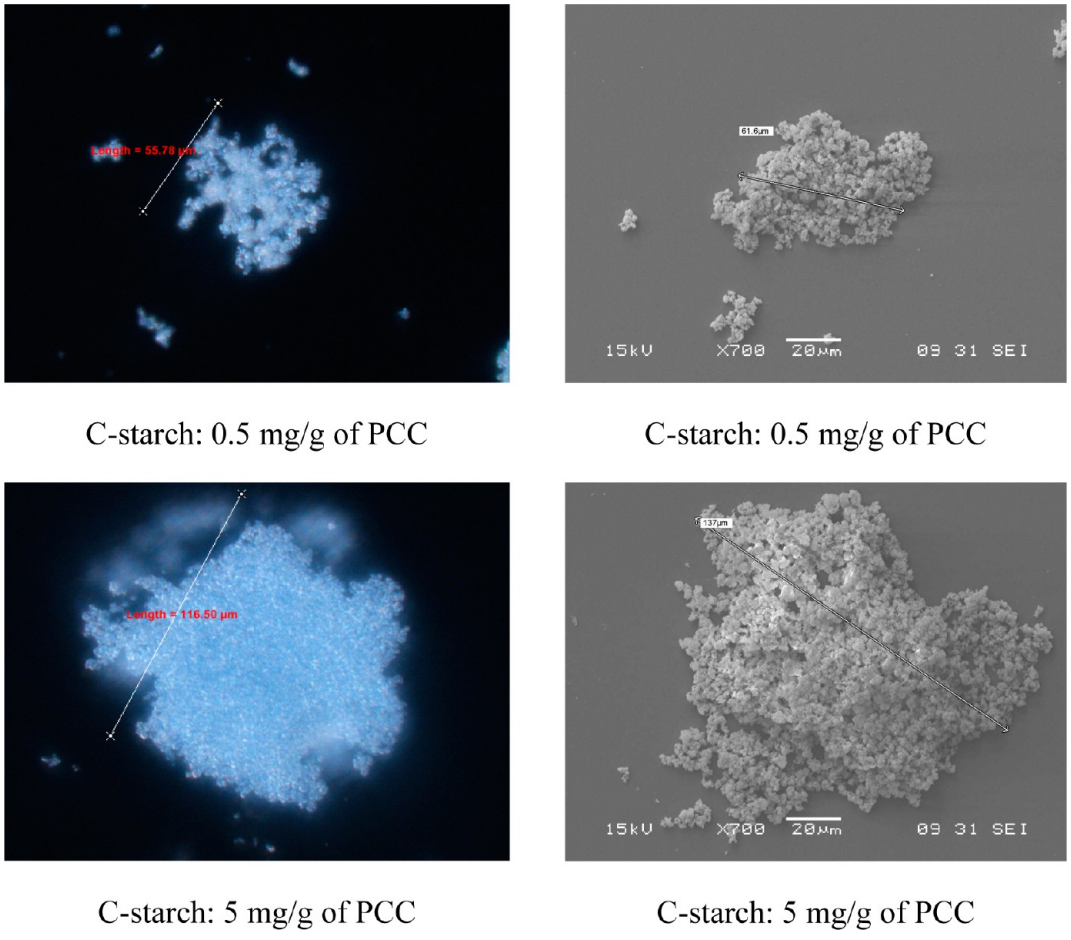

Figure 13. Optical (left) and SEM (right) images of PCC aggregates induced by C-starch. Top and bottom images show PCC aggregates produced from low and high C-starch dosages, respectively. The optical and SEM do not show the same aggregate.

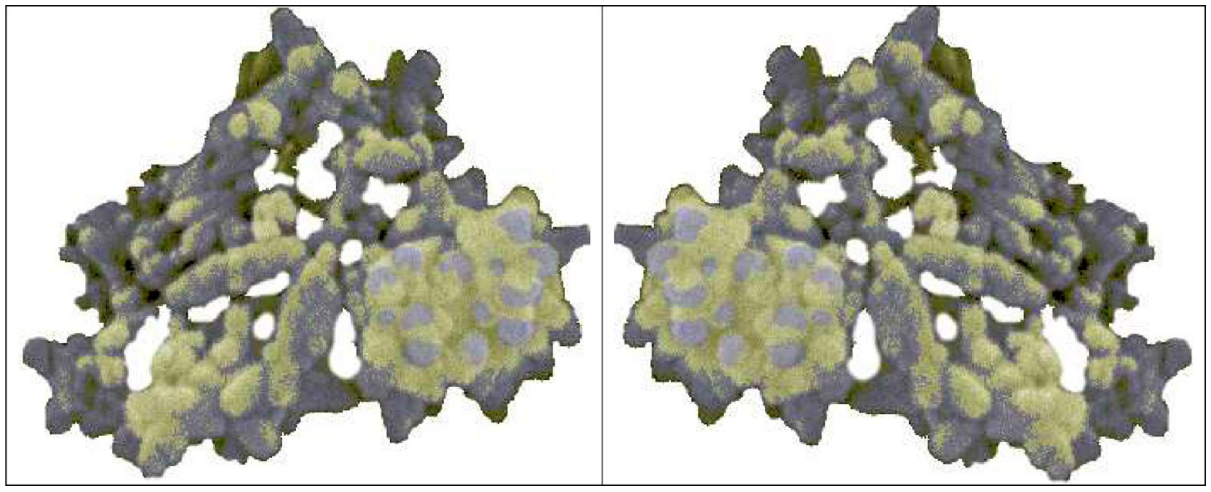

Figure 14. Cartoon showing PCC−PCC aggregation of real mirror images of a PCC particle: (1) The bridging surface area is much smaller that the projected area and (2) the top of the surface asperities (light green) are the bonding sites.

photometric dispersion analysis (PDA), image analysis, scanning electron microscopy (SEM), and light microscopy. RTFVI combined with image analysis was used to measure the number of discrete PCC particles in aggregates. This method has the potential of measuring polymer adsorption on particles. Using RTFVI, it was found that the fractional surface coverage in the area of observation by PCC aggregates increases linearly with time, with the slope determined by the size of the aggregates. PEO/cofactor induced aggregates were weaker at high shear and far more irreversible than those induced by PVFA/NaAA or C-starch. Flocs produced at low polymer dosages were smaller and weaker than those produced at higher dosages. Extension of this work to study the pH and salt dependence of weak polyelectrolytes would be of interest.

DOI: 10.1021/acs.iecr.5b00818
Ind. Eng. Chem. Res. XXXX, XXX, XXX−XXX

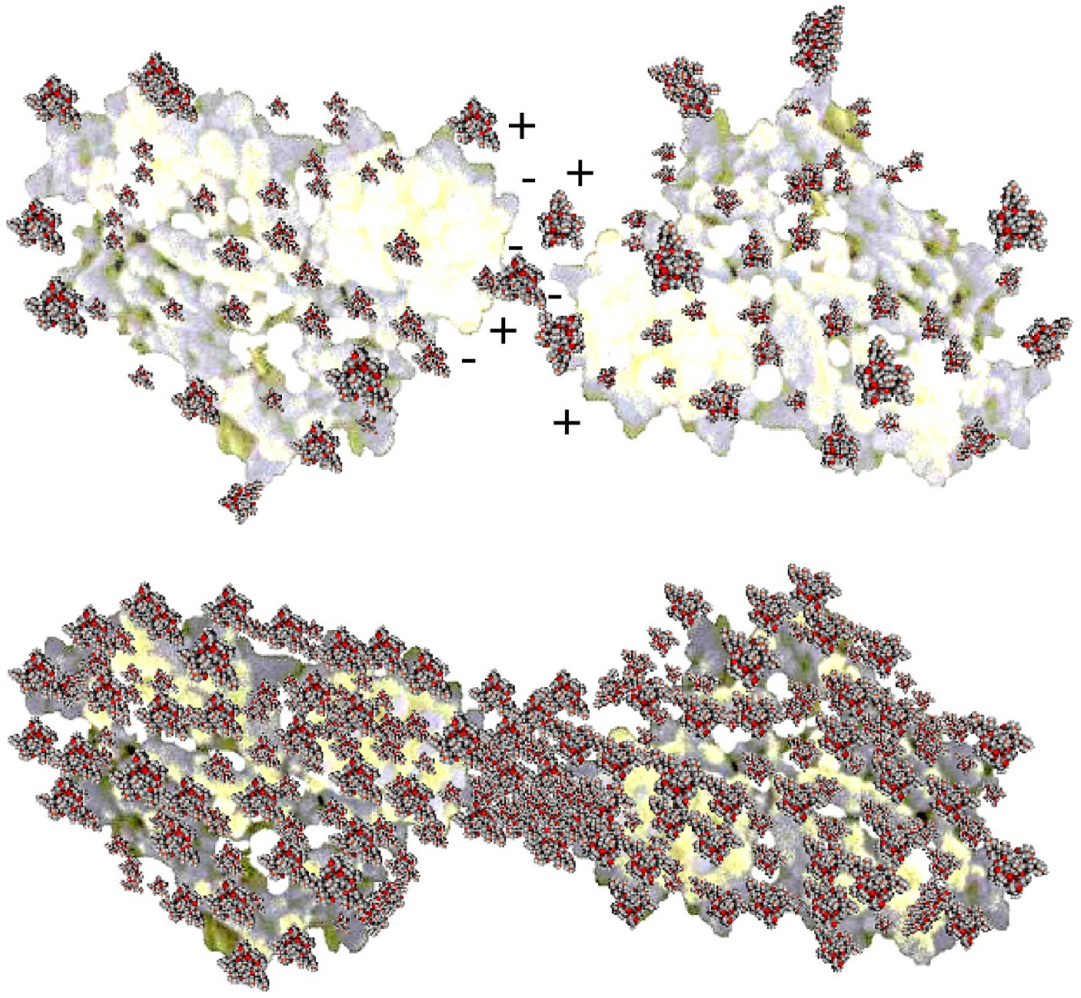

Figure 15. Effective surface area for polymer bridging. (Top) Classical bridging or charge neutralization flocculation. (Bottom) Additional polymer absorption results in higher coverage of the external and internal surfaces and prevents further aggregation due to electrosteric repulsion.

We speculate that when two scalenohedral crystal type PCC particles aggregate, there is a small effective surface area to bind them, mainly through classical bridging or charge neutralization flocculation. Moreover, additional polymer absorption results in higher coverage of the external and internal surfaces and prevents further aggregation due to electrosteric repulsion.

The implication of this finding is that that the experimental SSA, e.g., obtained from BET, cannot be used for the kinetic calculations because a significant amount of polymers is buried inside the scalenohedral crystal type PCC asperities. Moreover, in modifying fillers for papermaking applications, using polymers which cannot penetrate the porous interior structure would be more cost-effective.

AUTHOR INFORMATION

Corresponding Author

*E-mail: rgaudreault@cascades.com.

Notes

The authors declare no competing financial interest.

ACKNOWLEDGMENTS

The authors wish to acknowledge the valuable assistance from colleagues at Harvard University: Dr. Cliff Brangwynne, Dr. Gijsje Koenderink, Dr. Tomas Angelini, and Dr. Carlos Martinez for their assistance on fluorescence video imaging, Dr. Chanjoong Kim and Dr. Daniel Blair for valuable insights. The authors also thank Denis Berthiaume from Cascades Rolland Division and Pascal Allard for the papermaking process, Claude Tremblay for the scanning electron microscopy, Eric St-Pierre for laboratory assistance, and Frédérick Anctil for the image analyses, all from the Research and Development Centre of Cascades Inc. The authors also acknowledge permission from *The 14th FRC Symposium* to reproduce figures from ref 67. Financial support from NSERC and FPInnovations for an Industrial Research Chair is also acknowledged.

REFERENCES

(1) Scott, W.E. *Principles of Wet End Chemistry*; Tappi Press: Atlanta, 1996.

(2) Haruo, K. Industrial production of aragonite PCC using the causticizing process in kraft pulping. *Fillers and Pigments for Papermakers, Pira International Conference*, Lisbon, Spain, 2005, June 3rd–4th.

(3) Pouget, E. M.; Bomans; Paul, H. H.; Goos, J. A. C. M.; Frederik, P. M.; De With, G.; Sommerdijk; Nico, A. J. M. The initial stages of template-controlled $CaCO_3$ formation revealed by Cryo-TEM. *Science* **2009**, *323*, 1455.

(4) Gebauer, D.; Völkel, A.; Cölfen, H. Stable prenucleation calcium carbonate clusters. *Science* **2008**, *322*, 1819.

(5) Piana, S.; Raiteri, P.; Taylor, Z.; Hughes, Z. E.; Gale. J. D. Exploring the dynamics of aqueous interfaces. *Proceedings of the Fundamental & Applied Pulp & Paper Molecular Modelling Symposium*; Gaudreault, R.,

DOI: 10.1021/acs.iecr.5b00818
Ind. Eng. Chem. Res. XXXX, XXX, XXX−XXX

Whitehead, M. A., van de Ven, T. G. M., Eds.; Desktop Publishing: Montreal, Canada, August 24−26, 2005, pp 13−22.
(6) Beazley, K. M.; Petereit, H. Effect of China clay and calcium carbonate on paper properties. *Wochenbl. Papierfabr.* **1975**, *103*, 143.
(7) Beazley, K. M.; Dennison, S. R.; Taylor. J. H. The influence of mineral fillers on paper strength: Its mechanism and practical means of modification. In *Preprints ESPRA European Mtg.*, Maastricht, The Netherlands, 1975; p 217.
(8) Lindström, T.; Floren, T. The effect of filler particle size on the dry-strengthening effect of cationic starch wet-end addition. *Nordic Pulp Pap. Res. J.* **1987**, *4*, 142.
(9) Fiarchild, G. H. Increasing the filler content of PCC-filled alkaline papers. *Tappi J.* **1992**, *75*, 85.
(10) Fiarchild. G. H. PCC morphology and particle size effects in alkaline paper. *Preprints Intl. Conf. Advanced Materials*, Cancun, Mexico, 1995.
(11) Li, L.; Collis, A.; Pelton, R. A new analysis of filler effects on paper strength. *J. Pulp Pap. Sci.* **2002**, *28*, 267.
(12) Han, Y. R.; Seo, Y. B. Effect of particle shape and size of calcium carbonate on physical properties of paper. *J. Korea Tappi* **1997**, *29*, 7.
(13) Bown, R. Particle size, shape and structure of paper fillers and their effect on paper properties. *Pap. Technol.* **1998**, *39*, 44.
(14) Modgi, M.; McQuaid, M. E.; Englezos, P. SEM/EDX Analysis: A technique for *z*-direction mineral topography in paper. *Nordic Pulp Pap. Res. J.* **2006**, *21*, 659.
(15) Modgi, M.; McQuaid, M. E.; Englezos, P. SEM/EDX Analysis of *z*-direction distribution of mineral content in paper along the cross-direction. *Pulp Pap. Can.* **2006**, *107*, 48.
(16) Rolland du Roscoat, S.; Bloch, J.-F.; Thibault. X. Characterization of the 3D paper structure with X-Ray synchrotron radiation micro-tomography. *Advances in Paper Science and Technology, The 13th FRC Symposium*; Robinson College: Cambridge, 2005, p 901.
(17) Tanaka, A.; Hiltunen, E.; Niskanen, K. Inter-fiber bonding effects of beating, starch or filler. *Nordic Pulp Pap. Res. J.* **2001**, *16*, 306.
(18) Lindström, T.; Kolseth, P.; Näslund, P. The dry strengthening effect of cationic starch wet-end addition on filled papers. In *Papermaking Raw Materials. Trans VIIIth Fund. Res. Symp.*; Oxford, U.K., **1985**; Vol. *II*, p 589.
(19) Koper, G. J. M.; Vanerek, A.; van de Ven, T. G. M. Poly(Propylene Imine) dendrimers as retention aid for the deposition of calcium carbonate on pulp fibres. *J. Pulp Pap. Sci.* **1999**, *25*, 81.
(20) van de Ven, T. G. M.; Vanerek, A.; Garnier, G. Filling wet paper with the use of a secondary head box. *Ind. Eng. Chem. Res.* **2004**, *43*, 2280.
(21) Laleg. M. Mechanical pulp papers filled with precipitated calcium carbonate (PCC): Some effects and benefits. *Fillers & Pigments for Papermakers. Pira International Conference Proceedings*; Lisbon, Spain, June 3rd−4th, 2005.
(22) Laufmann. M. Calcium carbonate fillers in SCC paper. *Fillers & Pigments for Papermakers. Pira International Conference Proceedings*, Lisbon, Spain, 2005, June 3rd−4th.
(23) Subramanian. R. Precipitated calcium carbonate composite fillers: Characteristics and effect on fine paper properties. *Fillers & Pigments for Papermakers. Pira International Conference Proceedings*, Lisbon, Spain, June 3rd−4th 2005.
(24) Modgi, D.; Trigylidas, I.; Thorburn, Il.; Englezos, P. Retention of calcium carbonate in mechanical pulps with PEO/cofactor/coagulant and the role of hydrogen bonding interactions. *Pulp Pap. Sci.* **2004**, *30*, 11.
(25) Alince, B.; Porubska, J.; van de Ven, T. G. M. Ground and precipitated $CaCO_3$ deposition on fibre in the presence of PEO and kraft lignin. *Pap. Technol.* **1997**, *38*, 51.
(26) Vanerek, A.; Alince, B.; van de Ven, T. G. M. Interaction of calcium carbonate fillers with pulp fibres: Effect of surface charge and cationic polyelectrolytes. *Pulp Pap.* **2000**, *26*, 9.
(27) Asselman, T.; Alince, B.; Garnier, G.; van de Ven, T. G. M. Mechanism of polyacrylamide-bentonite—Microparticulate retention aids. *Nordic Pulp Pap. Res. J.* **2000**, *15*, 515.
(28) Alince, B.; Bednar, F.; van de Ven, T. G. M. Deposition of calcium carbonate particles on fiber surfaces induced by cationic polyelectrolyte and bentonite. *Eng. Aspects* **2001**, *190*, 71.
(29) Xu, Y.; Chen, X.; Pelton, R. How Polymers strengthen filled papers. *Tappi J.* **2005**, *4*, 8.
(30) Subramanian, R.; Maloney, T.; Paulapuro, H. Calcium carbonate composite fillers. *Tappi J.* **2005**, *4*, 23.
(31) Srivastsa, N. R.; Patnaik, S.; Hart, P.; Amidon, T. E.; Renard, J. J. Method for improving brightness and cleanliness of secondary fibers for paper and paperboard manufacture, U.S. Patent No. 5,665,205; September 9, 1997.
(32) Matthew, M. C.; Patnaik, S.; Hart, P.; Amidon, T. E. Process for enhanced deposition and retention of particulate filler on papermaking fibers, U.S. Patent No. 5,679,220; October 21, 1997.
(33) Cousin, L.; Mora, F.; Highly loaded fiber-based composite material, U.S. Patent No. 5,731,080; March 24, 1998.
(34) Cousin, L.; Mora, F.; Method of manufacture for highly loaded fiber-based composite material, U.S. Patent No. 5,824,364; October 20, 1998.
(35) Koukoulas, A. A.; Altman, T. E.; Matthew, M. C.; Amidon, T. E.; Mora, F. Method to manufacture paper using fiber filler complexes, U.S. Patent No. 6,592,712 B2; July 15, 2003.
(36) Jewell, R. A.; Neogi, A. N.; White, S. J. Method for increasing filler retention of cellulosic fiber sheets, U.S. Patent No. 6,514,384 B1; February 4, 2003.
(37) Jewell, R. A.; Neogi, A. N.; White, S. J. Method for increasing filler retention of cellulosic fiber sheets, U.S. Patent No. 6,824,649 B2; November 30, 2004.
(38) T. G. M. van de Ven. Filler and fines retention in papermaking. *Advances in Paper Science and Technology. The 13th FRC Symposium*; Pulp & Paper Fundamental Research Society: Bury Lancashire, U.K., Robinson College, Cambridge, September 11th−16th, 2005, pp 1193−1224.
(39) Modgi, M.; McQuaid, M. E.; Englezos, P. Interaction of precipitated calcium carbonate (PCC) with starch in distilled and de-ionised water (DDW) and process water (PW). *Nordic Pulp Pap. Res. J.* **2006**, *21*, 716.
(40) Sang, Y.; Englezos, P. Flocculation of precipitated calcium carbonate (PCC) by cationic tapioca starch with different charge densities. II: Population balance modeling. *Colloids Surf. A* **2012**, *414*, 520.
(41) Poraj-Kozminski, A.; Hill, R. J.; van de Ven, T. G. M. Flocculation of starch-coated solidified emulsion droplets and calcium carbonate particles. *J. Colloid Interface Sci.* **2007**, *309*, 99.
(42) van de Ven, T. G. M.; Alince, B. Association-Induced Polymer Bridging: New insights into the retention of fillers with PEO. *J. Pulp Pap. Sci.* **1996**, *22*, J257.
(43) van de Ven, T. G. M.; Alince, B. Heteroflocculation by asymmetric polymer bridging. *J. Colloid Interface Sci.* **1996**, *181*, 73.
(44) Fleer, G.J.; Cohen Stuart, M. A.; Scheutjens, J. M. H. M.; Cosgrove, T.; Vincent, B. *Polymers at Interfaces*; Chapman & Hall: London, 1993, 112.
(45) Gregory, J. The effect of cationic polymers on colloidal stability of latex particles. *J. Colloid Interface Sci.* **1976**, *55*, 35.
(46) LaMer, V. K.; Healy, T. W. Adsorption−flocculation reactions of macromolecules at the solid−liquid interface. *Rev. Pure Appl. Chem.* **1963**, *13*, 112.
(47) Fleer, G. J.; Lyklema, J. Polymer adsorption and its effect of the stability of hydrodynamics colloids II. The flocculation process as studied with the silver iodide-polyvinyl alcohol system. *J. Colloid Interface* **1974**, *46*, 1.
(48) Hubbe, M. A. Flocculation and redispersion of cellulosic fiber suspension: A review of effects of hydrodynamic shear and polyelectrolytes. *BioResources* **2007**, *2*, 296.
(49) Porubská, J.; Alince, B.; van de Ven, T. G. M. Homo and heteroflocculation of papermaking fines and fillers. *Colloids Surf. A* **2002**, *210*, 97.
(50) van de Ven, T. G. M. Orthokinetic heteroflocculation in papermaking. In *Highlights in Colloid Science*; Platikanov, D., Exerowa,

DOI: 10.1021/acs.iecr.5b00818
Ind. Eng. Chem. Res. XXXX, XXX, XXX−XXX

D., Eds.; Wiley-VCH Verlag GmbH & Co. KGaA: Weinheim, 2009; pp 1−12.
(51) Gaudreault, R.; van de Ven, T. G. M.; Whitehead, M. A. Mechanisms of flocculation with poly (ethylene oxide) and novel cofactors: Theory and experiment. *Colloids Surf. A* **2005**, *268*, 131.
(52) Weitz, D. A.; Oliveria, M. Fractal structures formed by kinetic aggregation of aqueous gold colloids. *Phys. Rev. Lett.* **1984**, *52*, 1433.
(53) Weitz, D. A.; Huang, J. S.; Lin, M. Y.; Sung, J. Dynamics of diffusion-limited kinetic aggregation. *Phys. Rev. Lett.* **1984**, *53*, 1657.
(54) Weitz, D. A.; Huang, J. S.; Lin, Y. L.; Sung, J. Limits of the fractal dimension for irreversible kinetic aggregation of fold colloids. *Phys. Rev. Lett.* **1985**, *54*, 1416.
(55) Weitz, D. A.; Lin, Y. L. Dynamic of cluster-mass distribution in kinetic colloid aggregation. *Phys. Rev. Lett.* **1986**, *57*, 2037.
(56) Lin, M. Y.; Lindsay, H. M.; Weitz, D. A.; Ball, R. C.; Klein, R.; Meakin, P. Universality in colloid aggregation. *Nature* **1989**, *339*, 360.
(57) Lin, M. Y.; Lindsay, H. M.; Weitz, D. A.; Klein, R.; Ball, R. C.; Meakin, P. Universal diffusion-limited colloid aggregation. *J. Phys.: Condens. Matter.* **1990**, *2*, 3093.
(58) Lin, M. Y.; Lindsay, H. M.; Weitz, D. A.; Ball, R. C.; Klein, R.; Meakin, P. Universal reaction-limited colloid aggregation. *Phys. Rev. A* **1990**, *41*, 2005.
(59) Weitz, D. A.; Lin, M. Y.; Lindsay, H. M. *Universality Laws in Coagulation*; Elsevier: Amsterdam, 1991; p 133.
(60) Lin, Y. L.; Klein, R.; Lindsay, H. M.; Weitz, D. A.; Ball, R. C.; Meakin, P. The structure of fractal colloidal aggregates of finite extent. *J. Colloid Interface Sci.* **1990**, *137*, 263.
(61) Gaudreault, R.; Di Cesare, N.; Weitz, D. A.; van de Ven, T. G. M. Flocculation kinetics of precipitated calcium carbonate. *Colloids Surf. A* **2009**, *340*, 56.
(62) Yilmaz, Y.; Alemdar, A. Fluoro-surfactant as a tool for both controlling and measuring the size of the organoclay aggregates. *Appl. Clay Sci.* **2005**, *30*, 154.
(63) Yeung, A. K. C.; Pelton, R. Micromechanics: A New Approach to Studying the Strength and Breakup of Flocs. *J. Colloid Interface Sci.* **1996**, *184*, 579.
(64) Yeung, A.; Gibbs, A.; Pelton, R. Effect of Shear on the Strength of Polymer-Induced Flocs. *J. Colloid Interface Sci.* **1997**, *196*, 113.
(65) Gibbs, A.; Pelton, R. Effect of PEO Molecular Weight on the Flocculation and Resultant Floc Properties of Polymer-Induced PCC Flocs. *J. Pulp Pap. Sci.* **1999**, *25*, 267.
(66) Gibbs, A.; Pelton, R.; Cong, R. J. The Influence of Dextran Derivatives on Polyethylene Oxide and Polyacrylamide-Induced Calcium Carbonate Flocculation and Floc Strength. *Colloids Surf. A* **1999**, *159*, 31.
(67) Gaudreault, R.; DiCesare, N.; van de Ven, T. G. M.; Weitz, D. A. The Structure and Strength of Flocs of Precipitated Calcium Carbonate Induced by Various Polymers used in Papermaking. In *Advances in Pulp & Paper Research, The 14th FRC Symposium*; St-Anne's College: Oxford, U.K., September 13th−18th, 2009, p 1193.
(68) Vanerek, A.; Alince, B.; van de Ven, T. G. M. Colloidal behaviour of ground and precipitated calcium carbonate fillers: Effects of cationic polyelectrolytes and water quality. *Pulp Pap.* **2000**, *26*, 135.
(69) Villegas-Jiménez, A.; Mucchi, A.; Whitehead, M. A. Ab initio molecular orbital investigation of the chemical interactions of water with the (10.4) calcite surface. *First Applied Pulp & Paper Molecular Modelling Symposium*; Gaudreault, R., Whitehead, M. A., van de Ven, T. G. M.; Eds.; Desktop Publishing: Montréal, Canada, August 24−26, 2005; pp 227−244, 2006.
(70) Suty, S.; Alince, B.; van de Ven, T. G. M. Stability of ground and precipitated $CaCO_3$ suspension in the presence of poly(ethylene imine) and salt. *J. Pulp Pap. Sci.* **1996**, *22*, J321.
(71) Gregory, J. Turbidity fluctuations in flowing suspensions. *J. Colloid Interface Sci.* **1985**, *105*, 357.
(72) Gregory, J.; Nelson, D. W. Monitoring of aggregates in flowing suspensions. *Colloids Surf.* **1986**, *18*, 175.
(73) Goto, S.; Pelton, R. The influence of phenolic cofactor on the properties of calcium carbonate flocs formed with PEO. *Colloids Surf. A* **1999**, *155*, 231.
(74) Firth, B. A. Flow properties of coagulated colloidal suspensions: II. Experimental properties of the flow curve parameters. *J. Colloids Interface Sci.* **1976**, *57*, 257.
(75) Firth, B. A.; Hunter, R. J. Flow properties of coagulated colloidal suspensions: III. The elastic floc model. *J. Colloid Interface Sci.* **1976**, *57*, 266.
(76) van de Ven, T. G. M.; Hunter, R. J. The energy dissipation in sheared coagulated sols. *Rheol. Acta* **1977**, *16*, 534.
(77) Serra, T.; Casamitjana, X. Structure of the aggregates during the process of aggregation and breakup under a shear flow. *J. Colloid Interface Sci.* **1998**, *206*, 505.
(78) Selomulya, C.; Amal, R.; Bushell, G.; Waite, T. D. Evidence of shear rate dependence on restructuring and breakup of latex aggregates. *J. Colloid Interface Sci.* **2001**, *236*, 67.
(79) Rasteiro, M. G.; Garcia, F. A. P.; Ferreira, P.; Blanco, A.; Negro, C.; Antunes, E. Evaluation of flocs resistance and reflocculation capacity using the LDS technique. *Powder Technol.* **2008**, *183*, 231.
(80) Peng, P.; Garnier, Gil. Effect of Cationic Polyacrylamide Adsorption Kinetics and Ionic Strength on Precipitated Calcium Carbonate Flocculation. *Langmuir* **2010**, *26*, 16949.

DOI: 10.1021/acs.iecr.5b00818
Ind. Eng. Chem. Res. XXXX, XXX, XXX−XXX